J Geod (2017) 91:933–944
DOI 10.1007/s00190-017-0997-y

ORIGINAL ARTICLE

Geocenter variations derived from a combined processing of LEO- and ground-based GPS observations

Benjamin Männel[1,2] · **Markus Rothacher**[1]

Received: 9 May 2016 / Accepted: 6 January 2017 / Published online: 31 January 2017

Abstract GNSS observations provided by the global tracking network of the International GNSS Service (IGS, Dow et al. in J Geod 83(3):191–198, 2009) play an important role in the realization of a unique terrestrial reference frame that is accurate enough to allow a detailed monitoring of the Earth's system. Combining these ground-based data with GPS observations tracked by high-quality dual-frequency receivers on-board low earth orbiters (LEOs) is a promising way to further improve the realization of the terrestrial reference frame and the estimation of geocenter coordinates, GPS satellite orbits and Earth rotation parameters. To assess the scope of the improvement on the geocenter coordinates, we processed a network of 53 globally distributed and stable IGS stations together with four LEOs (GRACE-A, GRACE-B, OSTM/Jason-2 and GOCE) over a time interval of 3 years (2010–2012). To ensure fully consistent solutions, the zero-difference phase observations of the ground stations and LEOs were processed in a common least-squares adjustment, estimating all the relevant parameters such as GPS and LEO orbits, station coordinates, Earth rotation parameters and geocenter motion. We present the significant impact of the individual LEO and a combination of all four LEOs on the geocenter coordinates. The formal errors are reduced by around 20% due to the inclusion of one LEO into the ground-only solution, while in a solution with four LEOs LEO-specific characteristics are significantly reduced. We compare the derived geocenter coordinates w.r.t. LAGEOS results and external solutions based on GPS and SLR data. We found good agreement in the amplitudes of all components; however, the phases in x- and z-direction do not agree well.

Keywords GPS · GRACE · GOCE · OSTM/Jason-2 · Geocenter · LEO orbit determination

✉ Benjamin Männel
benjamin.maennel@gfz-potsdam.de

[1] Institute of Geodesy and Photogrammetry, ETH Zurich, 8093 Zurich, Switzerland

[2] Present Address: Deutsches GeoForschungsZentrum GFZ, Telegrafenberg, 14473 Potsdam, Germany

1 Introduction

The origin of the International Terrestrial Reference System (ITRS) is conventionally defined to be at the center-of-mass (CM) of the whole Earth's system, including the solid Earth, the oceans, the atmosphere, the hydrosphere and the cryosphere (Petit and Luzum 2010). The International Terrestrial Reference Frame (ITRF) is a realization of the ITRS derived from a globally distributed network of geodetic stations attached to the surface of the solid Earth. The coordinates of these stations are defined such that the origin of the coordinate system, the center-of-figure (CF), has zero translation and translation rate relative to the CM on decadal time scales (Altamimi et al. 2011). Driven by mass redistributions, the CF varies on shorter time scales with predominant annual and semiannual periods relative to the CM (Dong et al. 2003). This motion is conventionally called geocenter motion, where CM is referred to as the geocenter (Petit and Luzum 2010).

To determine the precise location of the geocenter, various approaches are available, which can be divided into (1) inverse and (2) translational approaches. Inverse methods determine the geocenter motion indirectly from mass redistribution or surface displacements (Blewitt et al. 2001; Lavallée et al. 2006; Fritsche et al. 2010). The classical translational approaches are based on satellites orbiting the CM and geodetic stations located on the surface of the solid Earth

(Vigue et al. 1992; Eanes et al. 1997; Pavlis 1999; Cheng et al. 2013). A more detailed description of these approaches (typically done with SLR) can be found in Wu et al. (2012).

Within this paper, we focus on the second approach. In principle, all geodetic satellite observations connecting satellites orbiting the CM and receivers located on the surface of the solid Earth are related by the very general equation (Meindl et al. 2013):

$$D_r^i = |\mathbf{r}^i(t_e) - (\mathbf{R}_r(t_r) - \mathbf{G}(t_r))| + \epsilon. \quad (1)$$

Here, D_r^i is the distance measurement between a satellite i with the geocentric position $\mathbf{r}^i$ and a receiver r with a position $\mathbf{R}_r$ with respect to the origin of the reference system. Consequently, the vector $\mathbf{G}$ accounts for the position vector of the geocenter relative to the origin of the reference system. The time epochs are the emission time t_e and the receiving time t_r of the microwave signal or the reflection time for optical signals. The term ϵ contains signal delays, sensor offset, technique-specific biases and measurement noise. Commonly, the unambiguous Satellite Laser Ranging (SLR) observations to the spherical satellites LAGEOS and ETALON are used to determine the geocenter (Eanes et al. 1997; Pavlis 1999; Cheng et al. 2013). Presently, it is the sole technique to align the long-term origin of the ITRF to the CM (Altamimi et al. 2011). It has to be mentioned that the geocenter determination based on satellite geodetic observations is, in general, less accurate for the z-component than for the x- and y-component. The main reason for this is that the geocenter in x- and y-direction is defined by gravity and Earth rotation (the Earth rotation axis is defined to pass through the geocenter), whereas the z-direction is only defined by gravity. Since many years also the prospects of using the much denser networks of the Doppler Orbitography and Radiopositioning Integrated by Satellite (DORIS) and the Global Navigation Satellite Systems (GNSS) to derive the geocenter are investigated. Corresponding results show a relatively low accuracy of the geocenter z-component compared to SLR when using the translational approach. In the case of GNSS, this weakness is mainly the result of: (1) the reduced sensitivity with respect to the geocenter due to the orbit height, (2) the need to estimate epoch-wise clock offsets or, alternatively, to form double-differences (cf. Meindl et al. 2013), (3) the presence of ambiguities in the raw phase observations, (4) the necessity to estimate tropospheric zenith delays and (5) difficulties in modeling the effect of solar radiation pressure (SRP).

Concerning the satellite types, low Earth orbiters (LEOs) have been used for SLR and DORIS-based geocenter estimations for many years, whereas GNSS observations to these satellites with few exceptions have not been considered so far. In recent years, Kang et al. (2009) presented geocenter results derived from GRACE GPS observations and a global tracking network. By estimating the LEO orbits, geocenter and GPS-specific parameters, they derived geocenter positions with a remarkable quality. Haines et al. (2015) presented a GPS-only terrestrial reference frame including also GRACE GPS observations. They found a significant improvement of the geocenter z-component based on the addition of the GRACE observations. Based on simulations, Kuang et al. (2015) studied accuracy limitations for various tracking configurations including a combined processing of ground- and space-based GPS observations using the kinematic approach. König et al. (2015) presented geocenter results from a combination of LAGEOS and GRACE solutions. However, they concluded that neither the addition of GRACE-based GPS, SLR, nor K-band observations could improve their inverse geocenter solution derived from LAGEOS observations. The status of empirical once-per-revolution (OPR) parameters compensating unmodeled solar radiation pressure in the combination of ground-based GNSS and LAGEOS observations was discussed by Thaller et al. (2014). They concluded that constraining the D and Y radiation pressure parameters to zero, as recommended by Meindl et al. (2013) for GNSS, will prevent LAGEOS from exploiting its potential in the combined solution.

In this paper, we present geocenter results based on the combined processing of the GPS observations from a globally distributed tracking network and several LEOs with different altitudes over 3 years (2010–2012). The LEOs are both GRACE satellites, GOCE and OSTM/Jason-2, as described in the next section. Also in Sect. 2 an overview of the data used, the LEO orbit determination and the overall processing scheme is provided. The impact of additional LEOs, the setup of OPR parameters and non-tidal loading corrections on the derived geocenter is discussed in Sect. 3. In Sect. 4, the impact of the individual LEOs and their orbit characteristics are presented and the comparison against SLR results is shown in Sect. 5. Conclusions and an outlook are provided in Sect. 6.

2 Data and processing

2.1 Observation data

Within this section, we provide an overview of the processed ground and space-based observations and we introduce the LEO satellite missions considered here. A global GPS ground tracking network with a total of 53 well-distributed and (mostly) stable stations of the International GNSS Service (IGS) was selected (Fig. 1). For the GPS processing, we used final GPS products provided by the IGS analysis center CODE (Dach et al. 2009). More details concerning input data and parametrization are given in Table 3. As a poorly distributed tracking network limits the accuracy of the derived geocenter, Fig. 2 shows the percentage of stations

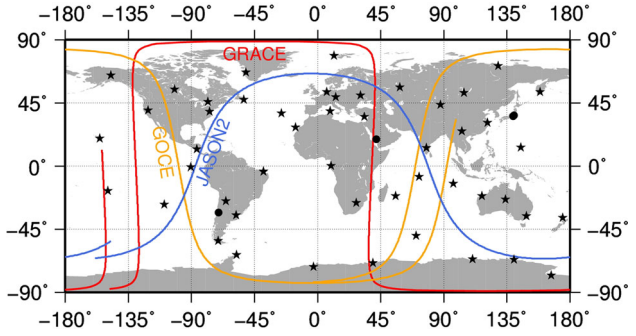

Fig. 1 Ground station network and LEO ground tracks (2010 Jan 1st, 0:00–2:00); *circles* indicate stations which were excluded from the NNT + NNR condition

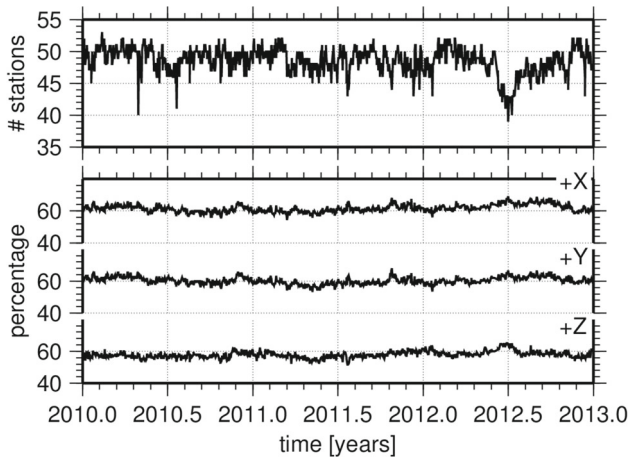

Fig. 2 Ground station network: number of stations in the combined solution (*top*) and percentage of stations in the $+x$(90° W to 90° E), $+y$(0° to 180° E) and $+z$(0° to 90° N) hemisphere

available in the $+x$(90° W to 90° E), $+y$(0° to 180° E) and $+z$(0° to 90° N) hemispheres. From Fig. 2, one can conclude that the distribution is not perfect, but acceptable. Concerning the network size, one has to keep in mind that weekly SLR solutions are usually based on around 20 stations,[1] whereas operational GNSS solutions comprise usually more than 100 stations.

Figure 1 also shows the ground tracks of the considered LEO missions. The satellite OSTM/Jason-2 is a follow-on of TOPEX/Poseidon and Jason-1 (Lambin et al. 2010) and was launched on June 28, 2008. The Jason-2 orbit follows the TOPEX/Poseidon orbit with a high altitude of 1336 km and an inclination of 66°. Beyond the Poseidon-3 radio altimeter, the satellite is equipped with a BlackJack GPS receiver, a DORIS antenna and a laser retro-reflector. The two GPS antennas (one for redundancy) are tilted around the satellite-fixed Y-axis by about 15° (Cerri and Ferrage 2015). Unfortunately, frequent receiver resets (mainly in the area of the South Atlantic Anomaly) resulted in a loss of tracking data (Cerri et al. 2010). The Gravity field and steady-state Ocean Circulation Explorer (GOCE, Floberghagen et al. 2011) was the first European Space Agency (ESA) Earth explorer core mission launched on March 17, 2009. One of the mission characteristics is the very low orbit (255 km during the first operation phase), which was a sun-synchronous dusk-dawn orbit with an inclination of 96.7°. To compensate for the atmospheric drag (and other non-gravitational forces), GOCE used an ion propulsion assembly. In addition to the three-axis accelerometer, a 12-channel GPS Lagrange receiver and a laser retro-reflector were carried by GOCE. After running out of fuel, GOCE reentered the Earth's atmosphere on November 11, 2013, after a very successful mission. The GRACE mission (Tapley et al. 2004) consists of two satellites orbiting the Earth in the same orbital trajectory separated by 220 ± 50 km. Both satellites were launched into an polar orbit with an inclination of 89° and an altitude of around 500 km on March 17, 2002. They are equipped with BlackJack GPS receivers, laser retro-reflector arrays and a K-band inter-satellite ranging system.

2.2 Precise orbit determination for LEOs

A reasonable combination of ground- and LEO-based GPS data requires the capability to perform a precise orbit determination (POD) for the considered LEOs. As we used the Bernese GNSS Software (BSW, Dach et al. 2015) for all the processing, the LEO orbit determination follows the scheme described by Jäggi et al. (2006), i.e., a reduced-dynamic approach is used. Besides the six Keplerian elements (a, e, i, Ω, ω, T_0) and nine empirical accelerations also pseudo-stochastic accelerations are estimated. In order to test the impact of a more dynamic orbit representation on the geocenter, the a priori modeling of solar radiation pressure and Earth albedo was implemented according to the work of Rodríguez-Solano (2014). The corresponding satellite-specific box-wing models were taken from Cerri et al. (2010) and Bettadpur (2012) for OSTM/Jason-2 and GRACE, respectively. For GOCE, we did not model non-gravitational forces a priori.

In Table 1, the average daily RMS values of the orbit differences between our (a priori) and external solutions are given. These differences are computed without estimating Helmert transformation parameters. The remaining differences of a few centimeters are caused by differences in the orbit representation model, the GPS products used and the a priori Earth rotation parameters. Results from an SLR validation, based on the difference between SLR observations and distances computed using fixed station coordinates and satellite orbits, are given in Table 2. The mean values over all resid-

[1] An averaged SLR station distribution of 60, 65 and 70% for the $+x$, $+y$ and $+z$ hemisphere is present in the weekly ILRS solution between 2010.0 and 2013.0.

Table 1 Orbit comparison: mean RMS values (cm) from differences between own and external solutions; orbit comparison without transformation; for comparison results from Flohrer et al. (2011) are added

LEO	Radial	Along	Cross	3D	Ref
GRACE-A	1.41	1.98	1.28	2.74	JPL[a]
GRACE-B	1.43	1.91	1.14	2.64	JPL[a]
GOCE	1.96	2.54	2.68	4.18	AIUB[b]
Jason-2	1.77	3.66	1.80	4.44	ESOC[c]
Jason-2	0.9	2.2	1.0		GDS3-JPL[d]
Jason-2	0.9	2.4	1.4		GDS3-CNES[d]

[a] GPS-only solution, GNV1B product, Bettadpur (2012)
[b] GPS-only solution, Bock et al. (2014)
[c] combined GPS, SLR, DORIS solution, Flohrer et al. (2011)
[d] 2008–2009, Flohrer et al. (2011)

Table 2 SLR validation; for comparison results from Bock et al. (2014) and Williams (2015) are added

	GRACE-A	GRACE-B	GOCE	Jason-2
# obs	59,565	60,870	17,939	345,541
Mean (cm)	−0.27	−0.35	−2.10	−0.07
RMS (cm)	2.69	2.70	3.68	2.88
Mean (cm)			0.18[b]	
RMS (cm)	2.00[a]	1.98[a]	1.84[b]	

[a] SLR validation of GNV1B orbits (Williams 2015)
[b] SLR validation 2009–2013, (Bock et al. 2014)

uals confirm the accuracy level shown in Table 1. However, for GOCE a—so far unexplained—systematic offset of 2 cm was found.

2.3 Data processing and combination

The processing work within this paper was done in a zero-difference mode using the Bernese GNSS Software. We choose the zero-difference mode (1) to ensure the maximal consistency between the ground network and the LEOs (by a joint estimation of GPS satellite clocks and orbits) and (2) to save the processing time that would be required for the rather complex ambiguity resolution between LEOs and ground stations. The major drawback is that with the BSW the ambiguities cannot be resolved at the zero-difference level. Therefore, only float solutions have been obtained. However, forming a consistent set of baselines between ground stations and LEOs and solving the ambiguities is quite a challenging task (c.f. Hugentobler et al. 2005). The possibility of forming baselines between LEOs was not considered as the three missions have significant differences in their orbit characteristics.

Our processing scheme includes three major steps: (1) preprocessing the LEO GPS data and a priori LEO orbit determination, (2) the preprocessing of the GPS ground tracking network and (3) the combined processing of all observations. To ensure the highest consistency in the last step, all observations have to contribute to the estimated parameters especially to the GPS satellite orbits and clocks, which are the connection between ground stations and LEOs. Before writing the normal equation system, a pre-elimination of epoch-wise clock corrections (due to their huge number) and either the LEO or the GNSS orbits (as the BSW cannot handle different orbit types at the normal equation level) is necessary. Therefore, all observations have to be processed in a huge least-squares adjustment (LSA). A station-wise processing and combination on the normal equation level would either reduce the consistency significantly by introducing several constraints especially in the satellite clocks or increase the processing load tremendously by keeping the epoch-wise satellite clocks in the normal equations. In addition, instead of LEO pseudo-stochastic accelerations pseudo-stochastic velocity changes were set up in the combined LSA, as BSW normal equation stacking, at present, cannot handle acceleration changes. Table 3 gives an overview of the a priori models and the parametrization used in the combined LSA. The normal equations derived are then solved to yield daily or accumulated to produce weekly solutions, while keeping the daily satellite arcs.

Figure 3 shows the average number of daily observations and the RMS of the carrier phase residuals for the processed stations and LEOs. The time span considered for these exemplary values is the 4 weeks of January 2010. The number of daily observations corresponds to 7–10 GPS satellites per epoch. The derived daily RMS values of the carrier phase residuals vary between 2.7 and 27.6 mm. In average, an RMS of 3.3 ± 0.3 mm and 11.5 ± 3.7 mm is derived for LEOs and ground stations, respectively. The differences between GRACE-A and GRACE-B are related to the slightly better quality of GRACE-B observations (cf. Montenbruck and Kroes 2003).

3 Geocenter results

Within this section, we will discuss the impact of (1) adding LEOs to the ground-only solution, (2) constraining empirical once-per-revolution parameters and (3) correcting non-tidal loading on the derived geocenter coordinates.

3.1 Impact of the inclusion of LEOs

Figure 4 shows the weekly geocenter time series obtained from the ground network (solution GR only). While variations in the x- and y-component are below 3 cm, they are up to 10 cm in the z-component. The variations in the z-component and their scatter (3.2 cm) are more than three

Table 3 Summary of estimation and processing strategy; GPS-related products serve as a priori information

Modeling and a priori information	
Base observations	Zero-difference phase observations, data rate: 30 s (ground stations) and 10 s (LEOs)
GPS-related products	Final products from CODE: orbits, 5-s clock corrections, Earth rotation parameters
LEO a priori orbit	Six Keplerian elements, nine empirical radiation pressure parameters, a priori SRP and Earth Albedo modeling for GRACE and OSTM/Jason-2
Troposphere modeling	6-hourly ECMWF-based hydrostatic troposphere delays mapped with VMF (Böhm et al. 2006)
Ionosphere modeling	Forming the ionosphere-free linear combination, accounting for second- and third-order, and ray-bending effects (Fritsche et al. 2005)
Antenna phase center	Absolute phase center offsets and variations for ground stations, GPS satellites, GOCE (Bock et al. 2011) and OSTM/Jason-2 (Garcia and Montenbruck 2007); GPS satellite antenna patterns beyond 14° from Schmid et al. (2016)
Gravity potential	EIGEN5C gravity field up to degree and order 120 (Förste et al. 2008)
Solid Earth tides	IERS 2010 conventions (Petit and Luzum 2010)
Permanent tide	Conventional tide free
Ocean tide model	FES2004 (Lyard et al. 2006)
Ocean loading	Tidal: FES2004 (Lyard et al. 2006), computed with the free ocean tide loading provider http://holt.oso.chalmers.se/loading/index.html
	Non-tidal: 6-hourly GRACE AOD1B atmospheric and oceanic de-aliasing product
Atmospheric loading	Tidal: S_1 and S_2 corrections from Ray and Ponte (2003) model
	Non-tidal: 6-hourly GRACE AOD1B atmospheric and oceanic de-aliasing product
Weighting	Ground and LEO observations are equally weighted
Parametrization	
Station coordinates	No-net-translation and no-net-rotation over 49 stations w.r.t. ITRF2008 (Altamimi et al. 2011)
GPS orbit modeling	Six orbital elements, nine empirical radiation pressure parameters (periodic components in D- and Y-direction are constrained with $1 \cdot 10^{12}$ nm/s^2) and three pseudo-stochastic pulses (velocities) per 12 h, a priori CODE radiation pressure model (Springer et al. 1999), arc length 24 h
LEO orbit modeling	Same as a priori, pseudo-stochastic pulses as velocity changes every six minutes
Geocenter	Freely estimated
Earth rotation	Rotation pole coordinates and UT1 for 24 h intervals, piece-wise linear modeling
Troposphere	13 zenith delays mapped with wet VMF and two gradients (east-west and north-south) mapped with Chen and Herring (1997) for every station and day
GPS satellite clocks	Pre-eliminated every epoch
Receiver clocks	Pre-eliminated every epoch
GPS phase center offset	Satellite-specific offsets per day, removed from the normal equations
Phase ambiguities	Pre-eliminated (as soon as possible)

times larger than the level reached by comparable results derived by SLR (cf. Sect. 5). The main reasons are most probably the sparse ground network (in terms of GNSS) and the unresolved ambiguities. However, when adding the four LEOs to the ground-only solutions (combined solution GR + ALL), variations decrease by a factor of about 2, i.e., to less than 2 cm (some peaks are larger, reaching up to 6 cm in the z-component) and even the scatter of the z-component is reduced to a value that is much closer to the SLR geocenter results (but it is still clearly larger than that of the SLR solutions). Also the amplitude spectra of all three components show significantly smaller amplitudes at nearly all frequencies. Also the predominant annual signals and the higher-order harmonics thereof, most probably related to the draconitic orbit period of GPS (351.4 days), are strongly reduced in the combined solution. However, our processed time span of 3 years does not allow to separate between annual and draconitic signals. The remaining annual signal is around 3 and 4 mm for the x- and y-component, respectively, and 6 mm for the z-component. For shorter periods, no significant signal common to all components can be found. Therefore, they might be related to ground network effects

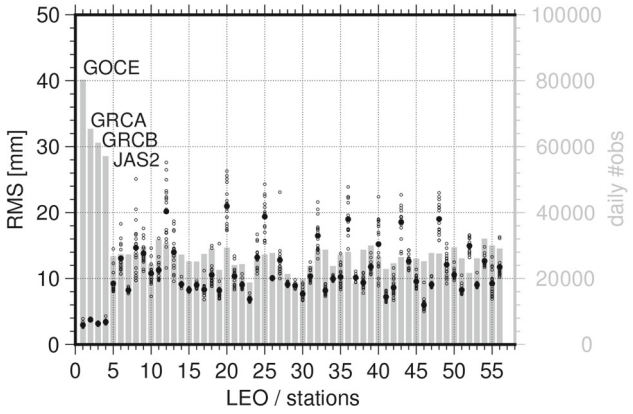

Fig. 3 Number of daily observations and RMS of phase residuals for all LEOs and stations (computed exemplarily over 4 weeks in 2010); data rate is 30 s for ground stations and 10 s for LEOs

and LEO orbit characteristics (see Sect. 4). The impact of the individual LEOs on the formal errors and the geocenter z-component is discussed in Sect. 4. As indicated in Fig. 4, GPS OPR orbit parameters are constrained in D- and Y-direction in both solutions. The impact of applying constraints to the GPS OPR terms is discussed in the next section.

3.2 Impact of empirical radiation pressure parameters

The free estimation of GPS OPR parameters parallel to the solar panel rotation axis (Y-direction) in the GNSS orbit determination process was identified by Meindl et al. (2013) as a major reason for the low accuracy of the geocenter Z-component by GNSS. However, as mentioned above, Thaller et al. (2014) recommend to freely estimate GPS OPR parameters when combining GNSS and LAGEOS for the geocenter determination. We computed two solutions with (1) free GPS OPR parameters and (2) constraining GPS OPR parameters in the direction toward the Sun (D-component) and parallel to the solar panel rotation axis (Y-component) to zero in the GNSS orbit determination process (as it was done by Thaller et al. (2014)). As the biggest effect is expected in the z-component, we show the resulting spectra in Fig. 5. Looking at the two ground-only solutions, the amplitudes of solution (2) are smaller for nearly all periods. As indicated in Fig. 4, an annual signal of 18 mm is derived from the ground network in solution (2), while this amplitude is increased to 20 mm in solution (1). A similar behavior is present in the semiannual amplitude (increase from 25 to 29 mm). In the GR + ALL solution, the annual amplitude is reduced to 6 mm in solution (2) with respect to the ground-only solution. When estimating GPS OPR freely in the GR + ALL solution, no annual peak is present. The estimated GPS OPR parameters have overall formal errors of $\approx$ 0.02 nm/s^2 and repeatabilities (weekly estimates compared to averaged values) of $\approx$ 1 nm/s^2. As mentioned in Sect. 1, constraining GPS OPR parameters has been found to be crucial for GNSS-based geocenter determination. This is also true for our experiment. The effect

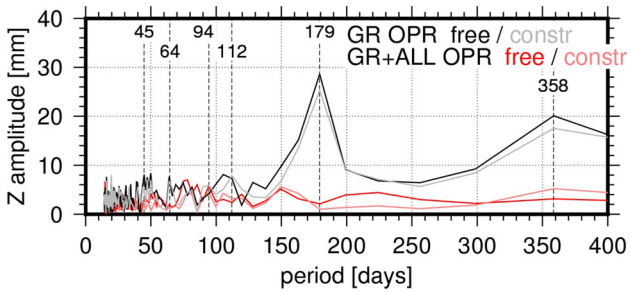

Fig. 5 Amplitude spectra of geocenter coordinates estimated in a ground-only and a combined processing with constrained and freely estimated empirical GPS OPR parameters; the periods of the major peaks are indicated

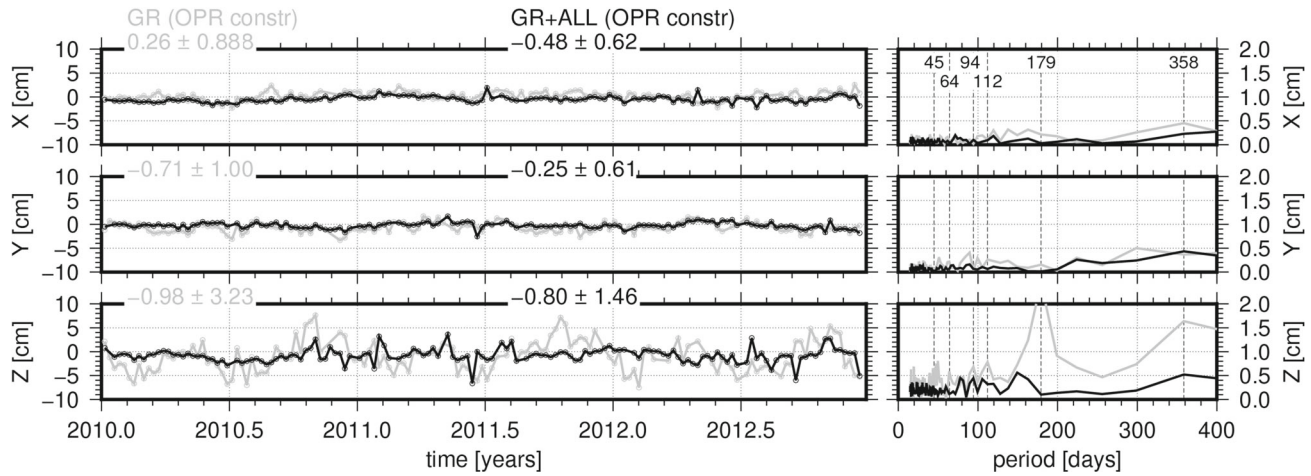

Fig. 4 Geocenter results from a ground-only (GR, *gray*) and a ground network + four LEO combination (GR + ALL, *black*) solution; *left*: time series; *right*: amplitude spectra; the periods of the major peaks are indicated

reported by Thaller et al. (2014) does not seem to be applicable for our LEO GPS observations, probably related (1) to the contribution the LEO GPS observations have to the GPS orbits and (2) to the large number of empirical LEO orbit parameters required to cope with air drag and radiation pressure. However, one has to keep in mind that in the applied zero-difference approach ambiguities have not been resolved to integers. Therefore, estimated ambiguities affect the derived geocenter results. For example, Brockmann (1997) reported for a GPS-based geocenter estimation an improvement by a factor of three due to fixed ambiguities.

Additionally, an accurate GPS orbit modeling becomes even more critical and the estimation of the full set of GPS OPR parameters might absorb remaining systematic effects. This needs to be tested in the future using the new CODE orbit model presented by Arnold et al. (2015). In the studies presented in the following, the GPS OPR parameters in *D*- and *Y*-direction have been constrained to zero.

3.3 Impact of non-tidal loading corrections

As indicated in Table 3, non-tidal loading effects were considered in the processing described above, as they affect the station coordinates. We applied the GRACE de-aliasing (AOD1B) products as they are used in Fritsche et al. (2014) to account for atmospheric and oceanic loading. To assess the impact of the corresponding displacements, we computed three solutions where (1) the AOD1B products were applied (GR + ALL(AOD)), (2) atmospheric non-tidal corrections provided by the GGOS atmosphere project (TU Vienna)[2] were applied (GR + ALL(TUV)) and (3) no non-tidal loading corrections were considered (GR + ALL(none)). Please note that non-tidal loading effects caused by the continental hydrology were not considered in any of these solutions. The geocenter time series differ by some mm in the horizontal components (not shown here) and by some cm in the *z*-component as shown in Fig. 6. Apart from periods with close agreement between the solutions, several weekly estimates show large differences compared to the results in the week before and after. A clear periodic (e. g. annual) behavior is not visible. The difference between results derived with AOD1B and TUV products amounts to up to 5 cm in the *z*-component, with slightly larger differences in the AOD1B case (due to considering ocean non-tidal loading). The spectral amplitudes plotted in Fig. 7 show a different behavior for short and long periods. For periods close to annual small differences of 0.6 and 1.5 mm are present between the GR + ALL(AOD) and the GR + ALL(TUV) solutions with respect to the solution without correcting for non-tidal loading (GR + ALL(none)). A bit strange is the larger signal for GR + ALL(TUV). However, the considered

[2] http://ggosatm.hg.tuwien.ac.at/, Dec.2015.

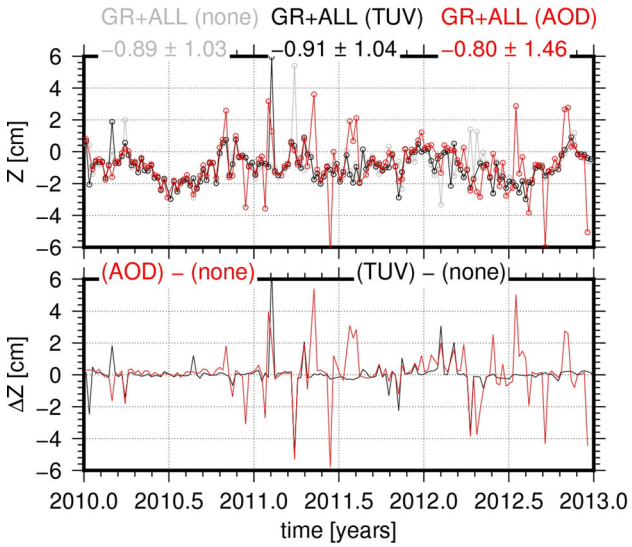

Fig. 6 Geocenter time series derived by a combined processing applying non-tidal loading corrections (*red*: using AOD1B products; *black*: using TU Vienna atmospheric non-tidal loading corrections); a solution without non-tidal loading corrections is shown in *gray*; corresponding differences are shown in the lower plot

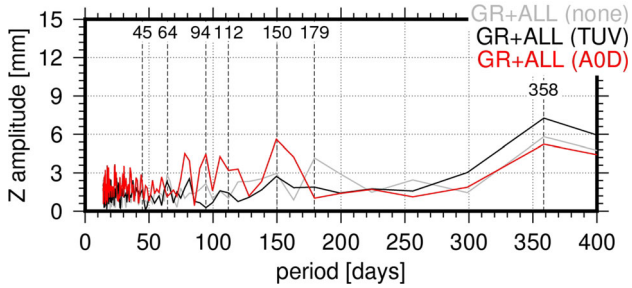

Fig. 7 Amplitude spectra of geocenter *z*-coordinate derived by a combined processing applying non-tidal loading corrections (*red*: using AOD1B products; *black*: using TU Vienna atmospheric non-tidal loading corrections); a solution without non-tidal loading corrections is shown in *gray*; the periods of the major peaks are indicated

3 years are a rather short time span to judge on annual signals. For periods shorter than 150 days, the GR + ALL(AOD) solution shows the largest amplitudes which are caused by several, in the absolute sense, large weekly estimates. In summary, we conclude that correcting for non-tidal loading for this type of geocenter determination is important. Studies performed by Sośnica (2015) and Roggenbuck et al. (2015) show a significant impact on the annual geocenter signal.

4 Comparing the impact of individual LEOs

In view of the geocenter improvement resulting from a combined processing of ground- and LEO-based GPS observations, the question arises how the individual satellites

Table 4 LEO characteristics: orbit and GPS equipment; altitude is given as approximation w.r.t. the processed time span

mission	Orbit		Receiver		Antenna	Remarks
	Altitude (km)	Inclination	Type	Channels		
GRACE	450	89°	BlackJack	10 (12)	Choke-ring	Two channels are switched off
GOCE	250	96.7°	LAGRANGE	12	Quadrifilar Helix	
OSTM/Jason-2	1336	66°	BlackJack	10	Choke-ring	Antenna tilted by 15°

contribute to this significant improvement. Obviously, the contribution depends on (1) the characteristics of the LEO orbit (e.g., the orbital inclination), (2) the quality and amount of the LEO GPS observations and (3) the quality and availability of additional information (e.g., attitude records). The second and third aspect can be treated together as they determine the quality of the derived LEO orbits. In the following, the individual contributions are discussed concerning the formal errors of the derived geocenter components and the behavior of the geocenter z-component is discussed.

4.1 Analysis of formal errors

Kuang et al. (2015) concluded that the formal errors of the geocenter estimation depend on (1) the altitude and inclination of the LEO orbital plane, (2) the orbit representation and (3) on the node differences, if two LEOs are processed simultaneously. As these findings are based on simulations, we attempt to complement them using real GPS observations of the LEO missions described above and in Table 4 (please note we did not study the impact of the orbit model). This approach is reasonable as the actual observation noise unique for each satellite is considered. Four conclusions can be obtained from the formal errors of the geocenter coordinates of daily and weekly solutions shown in Fig. 8. Firstly, the dramatic decrease from daily to weekly solutions is caused by a better separation of the correlated dynamic orbit parameters (kept as daily parameters) and the geocenter coordinates (estimated over 7 days). Secondly, adding a single LEO decreases the formal errors by about 20%, i.e., eight times more than the theoretical decrease expected due to the increased number of observations. Please note that due to the higher data rate, a LEO contributes three times more observations than a ground station. The total number of observations per day increases from approximately 1.27×10^6–1.34×10^6 for a ground + single-LEO combination. Thirdly, when adding more than one LEO, the formal errors decrease again by around 15% per additional LEO. And fourthly, this decrease depends as expected on the individual LEO. Unfortunately, we cannot assign these differences to the reasons mentioned above.

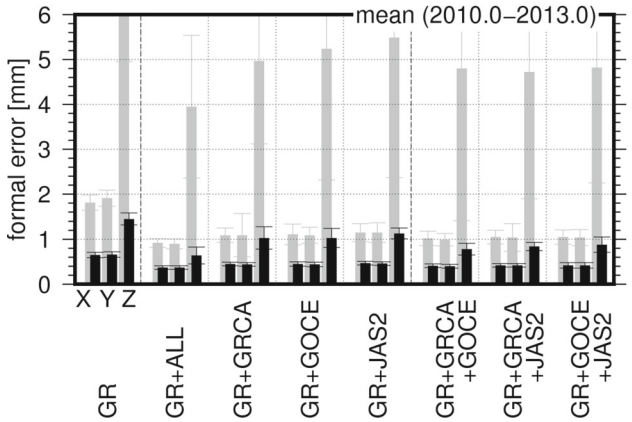

Fig. 8 Mean values of geocenter formal errors from daily (*gray*) and weekly (*black*) solutions

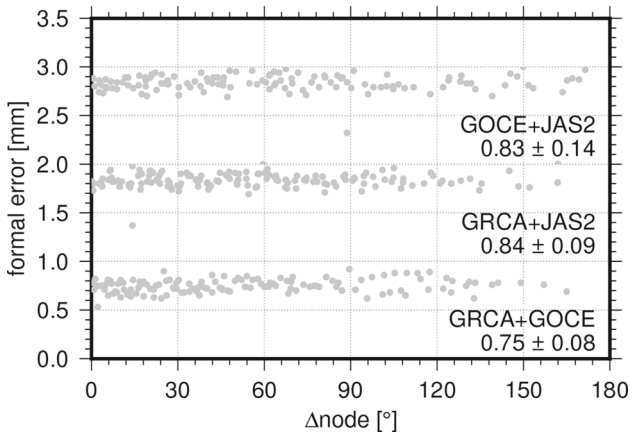

Fig. 9 Formal error of geocenter z-component from weekly dual-LEO solutions compared against the difference between the right ascension of the ascending nodes of the LEOs; all but GRCA + GOCE are vertically shifted by 1.0 mm w.r.t. each other

Kuang et al. (2015) also discussed the impact of the difference between the right ascension of the ascending nodes of the LEOs used on the geocenter formal errors. Based on their simulations they found a decrease of 0.1 mm in the formal error of the geocenter z-component for node differences of around 180°. In Fig. 9, we plotted the formal error of the weekly z-component for three different dual-LEO solutions. However, based on our results we could not confirm the decrease indicated by Kuang et al. (2015) as our results

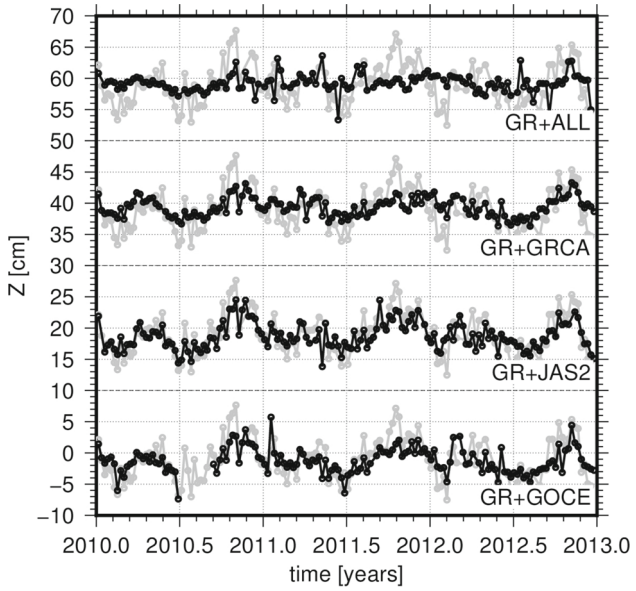

Fig. 10 Geocenter z-component time series derived by a combined processing: below three single-LEO solutions, at the *top* a solution containing all four LEOs with weekly solutions; for comparison the ground-only solution is shown in *gray*; all but *GR + GRCA* are vertically shifted by 20 cm w.r.t. each other

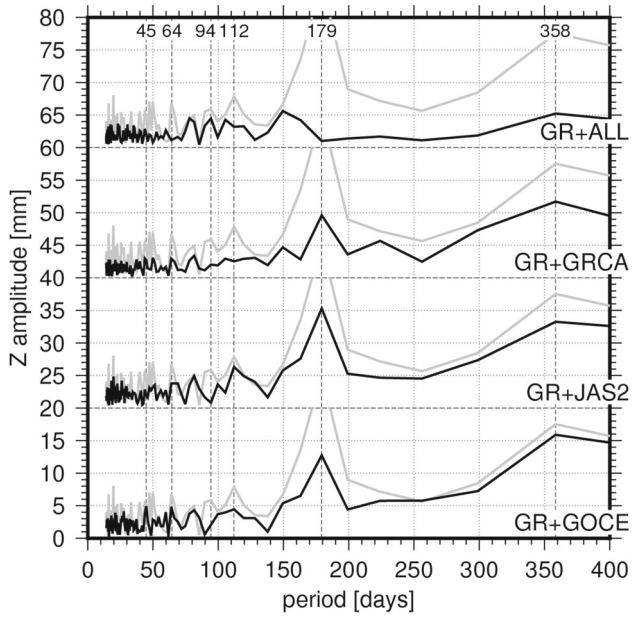

Fig. 11 Amplitude spectra of the geocenter z-coordinate estimated in a ground + LEO processing; the periods of the major peaks are indicated; for comparison the ground-only solution is shown in *gray*; all but *GR + GOCE* are vertically shifted by 20 mm w.r.t. each other

are probably too noisy and only few values are available for node differences larger than 150°.

4.2 Behavior of the geocenter *Z*-component

Figure 10 shows the geocenter z-component time series derived from weekly solutions based on three different ground network + single-LEO and one ground network + four-LEO (GR + ALL) combinations. Comparing against the ground-only solution in Fig. 4, it is obvious that some suspicious characteristics are disappearing (e.g., the peak at 2010.4 in GR + GRCA or the peak at 2012.45 in GR + JAS2), whereas others are mitigated but remain visible in all four solutions (e.g., the peak at 2011.35). The extent of the damping depends on the characteristics of the LEO orbit. Or, as the ground network distribution plays an important role, the damping depends also on the geometry between LEO trajectory and ground network (LEO-specific repeat orbit period). Compared to the ground-only solution, the time series are in general smoother but showing the same phases. Please note that due to missing GOCE GPS observations in summer 2010 (due to a telemetry problem) the GR + GOCE solution is missing between 2010.5 and 2010.7. In the amplitude spectra (Fig. 11), significant differences are visible at almost all periods. The nearly annual and semiannual amplitudes differ by up to 5 mm between the different single-LEO solutions (13, 11 and 16 mm are present for GR + GRCA, GR + GOCE and GR + JAS2, respectively). A strong response at annual and semiannual periods can be found in these single-LEO solutions, whereas both signals are strongly reduced in the GR + ALL solution. However, for this solution a 150-day peak is present which is not visible in the ground-only results (hidden in the edge of the semiannual signal) but in the single-LEO combination. In the GR + GRCA + GOCE solution (not shown here), the 179- and the 150-day signals have the same amplitude. In general, long-period signals are damped significantly in the GR + ALL solution. Therefore, we conclude that using several LEOs will strengthen the geocenter estimation by minimizing the effects of LEO-specific orbit characteristics on the geocenter results. For periods up to 130 days, the differences between the single-LEO solutions are related to the LEO characteristics (e.g., their draconitic period). These effects also remain in the GR + ALL solution.

5 Comparison to SLR results

As mentioned above, SLR is probably the technique mostly used to derive geocenter coordinates. In order to compare our results against SLR solutions, we selected two SLR solutions. The first one was derived at the Astronomical Institute of the University of Berne (AIUB) based on observations to LAGEOS-1 and LAGEOS-2 (Sośnica et al. 2015). The second one was computed in-house based on LAGEOS-1 and LAGEOS-2 observations using the Bernese GNSS Software. Figure 12 shows the three time series that are based on weekly solutions from the LAGEOS satellites (1) computed in-house, (2) computed by AIUB and (3) the GR + ALL geocenter results. A good agreement can be found in the x- and y-component, but the x-component of the GR + ALL solution

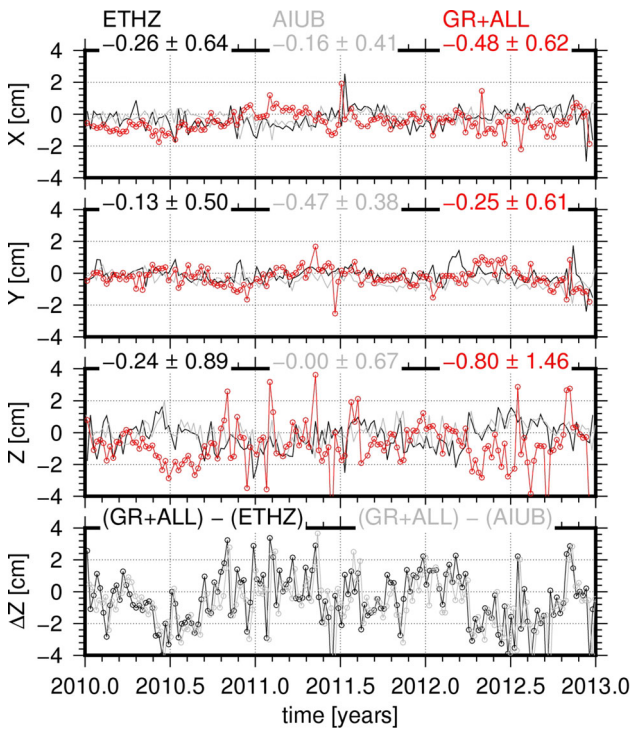

Fig. 12 Geocenter time series derived by a ground+LEO processing (GR+ALL, *red*) and SLR observations to LAGEOS in an in-house solution (ETHZ, *black*) and in the AIUB solution (*gray*); *bottom*: corresponding differences ETHZ-GR+ALL (*black*) and AIUB-GR+ALL (*gray*), respectively

seems to be significantly phase-shifted. For the most interesting z-component, the GR+ALL weekly results are relatively large compared to both SLR solutions. The corresponding differences, also shown in Fig. 12, are up to ±4 cm and show an annual periodic behavior. Concerning the scatter in the time series the accordance in the x- and y-component is quite good, whereas the scatter of the GR+ALL z-component is twice as large as the corresponding values for SLR. However, it should be kept in mind that (in terms of GNSS) a rather small ground network of approximately 50 stations was processed.

To characterize the annual signals in all three components, we estimated corresponding amplitudes A_i and phases ϕ_i. To determine these, we used a least-squares fit of a polynomial and trigonometric functions according to Kang et al. (2009), which reads as

$$C(t) = \sum_{i=1}^{n} A_i \sin\left(\frac{2\pi}{P_i}(t - t_0) + \phi_i\right) + b_0 + b_1(t - t_0). \tag{2}$$

In Eq. 2, the period is indicated by P_i, the time epoch t_0 is given by 1 January, and b_0 and b_1 are bias and trend, respectively. The derived amplitude and phase values for the GR+ALL and both SLR time series are summarized in Table 5 together with a choice of results found in the literature. First of all, the annual signal derived from our LAGEOS solution agrees well with other values published. However, the amplitude and phase uncertainties are comparably large as we considered only 3 years of data. The ground-only solution shows a good agreement in y-component but large amplitudes and different phases in the x- and z-component. The phase of the z-component is, however, comparable to

Table 5 Annual component of geocenter motion; amplitude (mm) and phase (°) of the annual signal (according to Eq. 2)

Reference	Data[b]	Time span	X		Y		Z	
			Amp.	Phase	Amp.	Phase	Amp.	Phase
Wu et al. (2006)[a,d]	GPS/OBP	1999.0–2004.2	1.7 ± 0.3	274 ± 11	3.8 ± 0.3	285 ± 4	4.5 ± 0.3	249 ± 4
Rietbroek et al. (2012)[a,d]	GPS/OBP	2003.0–2010.0	2.1	214	2.4	303	3.0	239
Cheng et al. (2013)[a]	SLR	1992.9–2011.0	2.7 ± 0.2	230 ± 2	2.8 ± 0.2	307 ± 2	5.2 ± 0.2	240 ± 3
Dong et al. (2003)	GPS	2000.2–2002.3	4.8 ± 0.4	220 ± 5	3.6 ± 0.4	320 ± 7	9.4 ± 0.5	105 ± 3
Fritsche et al. (2010)[a]	GNSS	1994.0–2008.0	0.1 ± 0.2	231 ± 92	1.8 ± 0.2	293 ± 11	4.0 ± 0.2	248 ± 6
Lavallée et al. (2006)[a]	GPS	1997.2–2004.2	2.1 ± 0.8	228 ± 21	3.2 ± 0.5	287 ± 22	3.9 ± 0.8	193 ± 2
Kang et al. (2009)	GPS/LEO	2003.0–2007.5	3.0 ± 0.2	244 ± 14	2.4 ± 0.2	286 ± 14	4.0 ± 0.2	344 ± 16
König et al. (2015)[a]	SLR/LEO	2006.0–2012.0	1.7 ± 0.6	210 ± 21	2.3 ± 0.8	341 ± 20	2.4 ± 0.8	220 ± 19
Rebischung and Garayt (2013)[a]	GPS	1997.0–2009.0	2.3	272	3.2	315	3.0	104
AIUB (Sośnica et al. 2015)[c]	SLR	2010.0–2013.0	1.6 ± 0.5	238 ± 22	2.1 ± 0.6	337 ± 12	3.1 ± 0.9	235 ± 19
This study (LAGEOS)	SLR	2010.0–2013.0	4.0 ± 0.8	231 ± 13	1.5 ± 0.7	309 ± 29	6.2 ± 0.9	265 ± 13
This study (GR only)	GPS/LEO	2010.0–2013.0	4.5 ± 1.0	103 ± 20	2.6 ± 1.3	297 ± 40	12.6 ± 3.7	112 ± 24
This study (GR+ALL)	GPS/LEO	2010.0–2013.0	3.2 ± 0.8	62 ± 19	4.0 ± 0.6	291 ± 14	5.9 ± 1.7	85 ± 26

[a] Phase results are converted to conform definition above
[b] Data: the used type of LEO data sets (GPS, SLR, K-band measurements, gravity data) can be found in the corresponding reference
[c] Computed from published time series
[d] Based on inverse geocenter approaches

the values derived by Dong et al. (2003) and Rebischung and Garayt (2013). The GR + ALL solution shows a better agreement in the amplitudes, where especially the z-amplitude is reduced to a realistic value. In the phase, only the y-component is comparable to the reference values; the values for x- and z-direction differ significantly from the values estimated by SLR, for example. However, as mentioned before, these disagreements might be related to (1) the zero-difference processing including (2) float ambiguities and (3) systematic effects due to solar radiation pressure. In any case, further investigations are needed to solve this issue.

6 Conclusion and outlook

We presented geocenter coordinate solutions derived in a combined zero-difference processing of ground network and LEO-based GPS observations. A well-distributed ground network of 53 stations and accurate LEO orbits, with an a priori accuracy of a few cm, were used. Firstly, we discussed the impact of the estimation of empirical once-per-revolution parameters for the GPS satellites. Based on our data, we conclude that OPR parameters (in D- and Y-direction) have to be constrained for a combined solution including LEO GPS data. Secondly, the importance of using non-tidal corrections was studied by applying GRACE AOD1B de-aliasing products and atmospheric non-tidal loading corrections provided by the GGOS atmosphere project at TU Vienna. Differences in the annual amplitude of around 0.5 mm w.r.t. a solution without non-tidal corrections encourage us to use the AOD1B products to correct for atmospheric and oceanic non-tidal loading effects. Thirdly, the impact of individual LEOs (GRACE-A, GOCE, OSTM/Jason-2) was discussed.

Adding one LEO to the ground-only processing decreases the formal errors by around 20% which is eight times more than the improvement expected due to the increased number of observations. Consequently, a huge improvement is found by adding the LEOs to the ground network in a combined processing. This shows the considerable potential of this combined approach. However, comparing our geocenter time series against SLR and comparing amplitudes and phases of an annual signal against external solutions shows some serious discrepancies. The main issues are the significant phase shifts in the x- and z-component. Further effort is needed to solve this issue. Especially resolving the phase ambiguities to their integer values would improve the derived solutions. Other deficiencies that are still present are the comparably small number of processed ground stations and the parametrization of the solar radiation pressure for the GPS case. To overcome the latter, we intend to introduce the new CODE model (Arnold et al. 2015). In summary, a combination of ground- and LEO-based GPS observations works at the zero-difference level quite well, a significant improvement compared to a ground network only solution was found, and the potential of a combined solution was shown. Concerning future geocenter studies, we plan to combine our GPS-based solutions with the presented LAGEOS geocenter solutions. In a second step, we intend to also add SLR observation to the LEO's involved.

Acknowledgements The authors want to thank IGS, ILRS, CODE, TU Vienna and the satellite missions GOCE, GRACE and OSTM/Jason-2 for providing the necessary observations and products. We would also like to thank three anonymous reviewers for their assistance in evaluating this paper and their helpful recommendations. This work was done within the projects SNF 200021E-160421 (funded by Swiss National Science Foundation) and "Co-location of Space Geodetic Techniques on Ground and in Space" which is part of the Deutsche Forschungsgemeinschaft funded research unit on reference systems (DFG FOR 1503).

References

Altamimi Z, Collilieux X, Métivier L (2011) ITRF2008: an improved solution of the international terrestrial reference frame. J Geod 85(8):457–473. doi:10.1007/s00190-011-0444-4

Arnold D, Meindl M, Beutler G, Dach R, Schaer S, Lutz S, Prange L, Sośnica K, Mervart L, Jäggi A (2015) Code's new solar radiation pressure model for gnss orbit determination. J Geod 89(8):775–791. doi:10.1007/s00190-015-0814-4

Bettadpur S (2012) Product specification document, 4.6 (edn). ftp://podaac.jpl.nasa.gov/allData/grace/docs/ProdSpecDoc_v4.6.pdf

Blewitt G, Lavallée D, Clarke P, Nurutdinov K (2001) A new global mode of earth deformation: seasonal cycle detected. Science 294(5550):2342–2345. doi:10.1126/science.1065328

Bock H, Jäggi A, Beutler G, Meyer U (2014) GOCE: precise orbit determination for the entire mission. J Geod 88(11):1047–1060. doi:10.1007/s00190-014-0742-8

Bock H, Jäggi A, Meyer U, Dach R, Beutler G (2011) Impact of GPS antenna phase center variations on precise orbits of the GOCE satellite. Adv Space Res 47(11):1885–1893. doi:10.1016/j.asr.2011.01.017

Böhm J, Werl B, Schuh H (2006) Troposphere mapping functions for GPS and VLBI from European Centre for medium-range weather forecasts operational analysis data. J Geophy Res 111(B2):B02406. doi:10.1029/2005JB003629

Brockmann E (1997) Combination of solutions for geodetic and geodynamical applications of the Global Positioning System (GPS). Geodätisch-geophysikalische Arbeiten in der Schweiz. Schweizerische Geodätische Kommission

Cerri L, Berthias JP, Bertiger WI, Haines BJ, Lemoine FG, Mercier F, Reis JC, Willis P, Zelensky NP, Ziebart M (2010) Precise orbit determination standards for the Jason series of altimeter missions. Mar Geod 33:379–418. doi:10.1080/01499419.2010.488966

Cerri L, Ferrage P (2015) DORIS satellites models implemented in POE processing. ftp://ftp.ids-doris.org/pub/ids/satellites/DORISSatelliteModels.pdf

Chen G, Herring T (1997) Effects of atmospheric azimuthal asymmetry on the analysis of space geodetic data. J Geophy Res 102(B9):20489–20502. doi:10.1029/97JB01739

Cheng M, Ries J, Tapley B (2013) Geocenter variations from analysis of SLR data. In: Altamimi Z, Collilieux X, (eds) Reference frames for applications in geosciences, volume 138 of IAG Symposia, pp 19–25. Springer, Berlin. doi:10.1007/978-3-642-32998-2_4

Dach R, Brockmann E, Schaer S, Beutler G, Meindl M, Prange L, Bock H, Jäggi A (2009) GNSS processing at CODE: status report. J Geod 83(3–4):353–366. doi:10.1007/s00190-008-0281-2

Dach R, Lutz S, Walser P, Fridez P (2015) Bernese GNSS Software Version 5.2. doi:10.7892/boris.72297

Dong D, Yunck T, Heflin M (2003) Origin of the international terrestrial reference frame. J Geophys Res. doi:10.1029/2002JB002035

Dow JM, Neilan RE, Rizos C (2009) The International GNSS service in a changing landscape of global navigation satellite systems. J Geod 83(3):191–198. doi:10.1007/s00190-008-0300-3

Eanes R, Kar S, Bettadapur S, Watkins M (1997) Low-frequency geocenter motion determined from SLR tracking. Eos Trans AGU 78:46

Floberghagen R, Fehringer M, Lamarre D, Muzi D, Frommknecht B, Steiger C, Piñeiro J, Da Costa A (2011) Mission design, operation and exploitation of the gravity field and steady-state ocean circulation explorer mission. J Geod 85(11):749–758. doi:10.1007/s00190-011-0498-3

Flohrer C, Otten M, Springer T, Dow J (2011) Generating precise and homogeneous orbits for Jason-1 and Jason-2. Adv Space Res 48:152–172. doi:10.1016/j.asr.2011.02.017

Förste C, Flechtner F, Schmidt R, Stubenvoll R, Rothacher M, Kusche J, Neumayer H, Biancale R, Lemoine J, Barthelmes F et al (2008) EIGEN-GL05C-A new global combined high-resolution GRACE-based gravity field model of the GFZ-GRGS cooperation. Geophys Res Abstr 10:EGU2008-A

Fritsche M, Dietrich R, Knöfel C, Rülke A, Vey S, Rothacher M, Steigenberger P (2005) Impact of higher-order ionospheric terms on GPS estimates. Geophy Res Lett. doi:10.1029/2005GL024342

Fritsche M, Dietrich R, Rülke A, Rothacher M, Steigenberger P (2010) Low-degree earth deformation from reprocessed GPS observations. GPS solut 14(2):165–175. doi:10.1007/s10291-009-0130-7

Fritsche M, Sośnica K, Rodríguez-Solano CJ, Steigenberger P, Wang K, Dietrich R, Dach R, Hugentobler U, Rothacher M (2014) Homogeneous reprocessing of GPS, GLONASS and SLR observations. J Geod 88(7):625–642. doi:10.1007/s00190-014-0710-3

Garcia M, Montenbruck O (2007) TerraSAR-X/TanDEM-X GPS Antenna Phase Center Analysis and Results. Space Flight Technology, German Space Operations Center, TN 07-03

Haines BJ, Bar-Sever YE, Bertiger WI, Desai SD, Harvey N, Sibois AE, Weiss JP (2015) Realizing a terrestrial reference frame using the global positioning system. Geophys Res Lett. doi:10.1002/2015JB012225

Hugentobler U, Jäggi A, Schaer S, Beutler G (2005) Combined processing of GPS data from ground station and LEO receivers in a global solution. In: Sansó F (ed) A window on the future of Geodesy. Springer, Berlin, pp 169–174. doi:10.1007/3-540-27432-4_30

Jäggi A, Hugentobler U, Beutler G (2006) Pseudo-stochastic orbit modeling techniques for low-Earth orbiters. J Geod 80(1):47–60

Kang Z, Tapley B, Chen J, Ries J, Bettadpur S (2009) Geocenter variations derived from GPS tracking of the GRACE satellites. J Geod 83(10):895–901. doi:10.1007/s00190-009-0307-4

König R, Dahle C, Vei M, Neumayer K-H (2015) A geocenter time series from a combination of LAGEOS and GRACE observations. IAG Symposia, pp 1–6. Springer, Berlin. doi:10.1007/1345_2015_24

Kuang D, Bar-Sever Y, Haines B (2015) Analysis of orbital configurations for geocenter determination with GPS and low-Earth orbiters. J Geod 89(5):471–481. doi:10.1007/s00190-015-0792-6

Lambin J, Morrow R, Fu L-L, Willis JK, Bonekamp H, Lillibridge J, Perbos J, Zaouche G, Vaze P, Bannoura W et al (2010) The OSTM/Jason-2 mission. Mar Geod 33(S1):4–25. doi:10.1080/01490419.2010.491030

Lavallée DA, Dam TV, Blewitt G, Clarke PJ (2006) Geocenter motions from GPS: a unified observation model. Geophy Res Lett 111(B5):B05405. doi:10.1029/2005JB003784

Lyard F, Lefevre F, Letellier T, Francis O (2006) Modelling the global ocean tides: modern insights from FES2004. Ocean Dyn 56(5–6):394–415. doi:10.1007/s10236-006-0086-x

Meindl M, Beutler G, Thaller D, Dach R, Jäggi A (2013) Geocenter coordinates estimated from GNSS data as viewed by perturbation theory. Adv Space Res 51:1047–1064. doi:10.1016/j.asr.2012.10.026

Montenbruck O, Kroes R (2003) In-flight performance analysis of the CHAMP BlackJack receiver. GPS Solut 7:74–86. doi:10.1007/S10291-003-0055-5

Pavlis E (1999) Fortnightly resolution geocenter series: a combined analysis of Lageos 1 and 2 SLR data. IERS Tech Note 25:75–84

Petit G, Luzum B (2010) IERS Conventions (2010). IERS Tech Note 36. Verlag des Bundesamts fr Kartographie und Geodäsie, Frankfurt am Main. ISBN 3-89888-989-6

Ray R, Ponte R (2003) Barometric tides from ECMWF operational analyses. Ann Geophys 21(8):1897–1910

Rebischung P, Garayt B (2013) Recent results from the igs terrestrial frame combinations. In: Altamimi Z, Collilieux X, (eds) Reference frames for applications in geosciences, volume 138 of IAG Symposia, pp 69–74. Springer, Berlin. doi:10.1007/978-3-642-32998-2_12

Rietbroek R, Fritsche M, Brunnabend S-E, Daras I, Kusche J, Schröter J, Flechtner F, Dietrich R (2012) Global surface mass from a new combination of GRACE, modelled OBP and reprocessed GPS data. J Geodyn 59–60:64–71. doi:10.1016/j.jog.2011.02.003

Rodríguez-Solano CJ (2014) Impact of non-conservative force modeling on GNSS satellite orbits and global solutions. Dissertation, Technische Universität München, München

Roggenbuck O, Thaller D, Engelhardt G, Franke S, Dach R, Steigenberger P (2015) Loading-induced deformation due to atmosphere, ocean and hydrology: model comparisons and the impact on global SLR, VLBI and GNSS solutions, pp 1–7. Springer, Berlin. doi:10.1007/1345_2015_214

Schmid R, Dach R, Collilieux X, Jäggi A, Schmitz M, Dilssner F (2016) Absolute IGS antenna phase center model igs08.atx: status and potential improvements. J Geod 90(4):343–364. doi:10.1007/s00190-015-0876-3

Sośnica K (2015) Determination of precise satellite orbits and geodetic parameters using satellite laser ranging. Geodätisch-geophysikalische Arbeiten in der Schweiz. Schweizerische Geodätische Kommission. http://boris.unibe.ch/53915/

Sośnica K, Jäggi A, Meyer U, Thaller D, Beutler G, Arnold D, Dach R (2015) Time variable Earth's gravity field from SLR satellites. J Geod. doi:10.1007/s00190-015-0825-1

Springer T, Beutler G, Rothacher M (1999) A new solar radiation pressure model for GPS satellites. GPS Solut 2(3):50–62. doi:10.1007/PL00012757

Tapley BD, Bettadpur S, Ries JC, Thompson PF, Watkins MM (2004) GRACE measurements of mass variability in the Earth system. Science 305(5683):503–505

Thaller D, Sośnica K, Dach R, Jäggi A, Beutler G, Mareyen M, Richter B (2014) Geocenter coordinates from GNSS and combined GNSS-SLR solutions using satellite co-locations. In: Earth on the edge: science for a sustainable planet, pp 129–134. Springer, Berlin. doi:10.1007/978-3-642-37222-3_16

Vigue Y, Lichten SM, Blewitt G, Heflin MB, Malla RP (1992) Precise determination of Earth's center of mass using measurements from the global positioning system. Geophys Res Let 19(14):1487–1490

Williams H (2015) Validating the 1-cm orbit. Master's thesis, University of Texas, Austin

Wu X, Heflin MB, Ivins ER, Fukumori I (2006) Seasonal and interannual global surface mass variations from multisatellite geodetic data. J Geophys Res. doi:10.1029/2005JB004100

Wu X, Ray J, van Dam T (2012) Geocenter motion and its geodetic and geophysical implications. J Geodyn 58:44–61. doi:10.1016/j.jog.2012.01.007